JBC RESEARCH ARTICLE

Metformin inhibits MAPK signaling and rescues pancreatic aquaporin 7 expression to induce insulin secretion in type 2 diabetes mellitus

Received for publication, January 19, 2021, and in revised form, July 15, 2021 Published, Papers in Press, July 22, 2021,
https://doi.org/10.1016/j.jbc.2021.101002

Xueting He[1,‡], Fei Gao[2,‡], Jiaojiao Hou[1,‡], Tingjie Li[1], Jiang Tan[1], Chunyu Wang[1], Xiaoyan Liu[1], Maoqi Wang[1], Hui Liu[1], Yuqin Chen[3], Zhuoyuan Yu[2], and Mei Yang[1,*]

From the [1]Department of Anatomy, College of Basic Medicine, [2]Department of Urology, The First Affiliated Hospital, [3]Institute of Neuroscience, College of Basic Medicine, Chongqing Medical University, Chongqing, People's Republic of China

Edited by Qi-Qun Tang

Metformin is the first-line antidiabetic agent for type 2 diabetes mellitus (T2DM) treatment. Although accumulated evidence has shed light on the consequences of metformin action, the precise mechanisms of its action, especially in the pancreas, are not fully understood. Aquaporin 7 (AQP7) acts as a critical regulator of intraislet glycerol content, which is necessary for insulin production and secretion. The aim of this study was to investigate the effects of different doses of metformin on AQP7 expression and explore the possible mechanism of its protective effects in the pancreatic islets. We used an *in vivo* model of high-fat diet in streptozocin-induced diabetic rats and an *in vitro* model of rat pancreatic β-cells (INS-1 cells) damaged by hyperglycemia and hyperlipidemia. Our data showed that AQP7 expression levels were decreased, whereas p38 and JNK mitogen-activated protein kinases (MAPKs) were activated *in vivo* and *in vitro* in response to hyperglycemia and hyperlipidemia. T2DM rats treated with metformin demonstrated a reduction in blood glucose levels and increased regeneration of pancreatic β-cells. In addition, metformin upregulated AQP7 expression as well as inhibited activation of p38 and JNK MAPKs both *in vivo* and *in vitro*. Overexpression of AQP7 increased glycerol influx into INS-1 cells, whereas inhibition of AQP7 reduced glycerol influx, thereby decreasing subsequent insulin secretion. Our findings demonstrate a new mechanism by which metformin suppresses the p38 and JNK pathways, thereby upregulating pancreatic AQP7 expression and promoting glycerol influx into pancreatic β-cells and subsequent insulin secretion in T2DM.

Metformin is a widely used antidiabetic drug for treating type 2 diabetes mellitus (T2DM) that enhances insulin regulation of glucose, promotes weight loss, and reduces appetite (1–3). These effects are generally explained by an increase in peripheral insulin sensitivity, and hence a decrease in blood glucose levels rather than a direct promotion of pancreatic insulin release. Overall, although metformin has been used as a drug for more than half a century, its antidiabetic mechanisms, particularly in the pancreas, have not been much documented (4).

Glycerol is metabolized in the pancreas and shows the potential to stimulate insulin production and secretion (5). Aquaporins comprise a family of 13 members of water channels (AQP0-12) that facilitate the rapid transport of water across cell membranes. In some cases, these pores are also permeated by small solutes, particularly solutes such as glycerol, urea, or nitric oxide, which are known as aquaglyceroporins. AQP7, a member of aquaglyceroporin family, is expressed in pancreatic β-cells, and murine studies have confirmed its participation in insulin secretion, triacylglycerol synthesis, and proliferation of these endocrine cells. Therefore, AQP7 is now considered as a β-cell protein and critical regulator of intraislet glycerol content (6). However, nothing is known about whether metformin could regulate this member protein in pancreatic islets and its possible mechanism.

Several molecular abnormalities are linked to T2DM, in which mutations in important regulatory networks remain substantial (7–9). Pancreatic β-cell injury and insulin resistance appear to be partially triggered by inflammatory (10), oxidative (11), and endoplasmic reticulum stress-induced pathways (12), including the mitogen-activated protein kinases (MAPK) signaling cascade. However, whether MAPK modulations affect AQP7 expression in pancreatic tissue of T2DM treated with metformin remains poorly understood. The present study aimed to investigate whether metformin improves and alleviates the symptoms through modulation of AQP7 and the MAPK pathway in pancreas of T2DM.

Results

Changes in the serum levels of glucose, triglycerides, and total cholesterol

Significant increases were observed for glucose (Glu), triglycerides (TG), and total cholesterol (TC) in the T2DM group compared with the normal control group (Ctrl) group ($p < 0.05$). After metformin (Met) treatment, serum Glu, TG, and TC were significantly decreased in T2DM+metformin (Met) groups [T2DM+M1 (100 mg/kg/d), T2DM+M2 (300 mg/kg/d)

‡ These authors contributed equally to this work.
* For correspondence: Mei Yang, yangmei503@cqmu.edu.cn.

and T2DM+M3 (500 mg/kg/d)] compared with the T2DM + 0.9% NaCl group (T2DM+NS) ($p < 0.05$ for all; Table S1), supporting the beneficial effects of metformin on the treatment of T2DM.

Metformin normalizes T2DM-induced histopathologic changes of pancreas

The pancreatic sections stained with hematoxylin and eosin (HE) are shown in Fig. S1. In the control group (Ctrl), pancreatic islet was normal without edema or inflammatory cells infiltration. In contrast, islets in the T2DM group showed disturbed cellular arrangement, necrotic changes in islets (karyolysis and loss of nuclei), and smaller islet cell masses. All these changes were alleviated in the T2DM+Met groups by metformin, especially in T2DM+M2 and T2DM+M3 group.

AQP7 colocalizes with insulin-producing cells and metformin normalized T2DM-induced downregulation of AQP7

We examined whether metformin could regulate AQP7 expression. To confirm AQP7 expression in the pancreas, we used immunohistochemistry to localize AQP7 and insulin in the pancreas by fluorescence microscopy and detected immunoreactive AQP7 in insulin-producing cells. Immunohistochemical staining of pancreatic tissues from the Ctrl group showed fairly well immunoreactive AQP7 in insulin-producing cells. However, immunostaining sample of T2DM group, T2DM+NS group, or T2DM+M1 group stained faintly for the few immunoreactive insulin-positive cells. On the contrary, immunostaining with AQP7 antibody in the T2DM+M2 group and T2DM+M3 group detected more intense immunostaining in insulin-positive cells than T2DM+NS group (Fig. 1).

To determine whether metformin had effects on AQP7 expression, western blot analysis was performed using pancreatic islets from all experimental groups. A significant reduction of AQP7 levels was noted in the T2DM group as compared with the Ctrl group ($p < 0.05$). An increase of AQP7 expression was observed in Met treatment groups in a dose-dependent manner, except for low-dose Met group (T2DM+M1) ($p < 0.05$) (Fig. 2, *A* and *B*).

In vitro, we established a glucolipotoxicity (0.25 mM palmitate and 33 mM glucose conditions) model in INS-1 cells based on previous studies (13–15). As shown, similar to the observations *in vitro*, INS-1 cells cultured under glucolipotoxicity conditions resulted in a significant reduction of AQP7 protein expression, which was markedly increased in the presence of 0.5, 1, and 2 mM metformin, respectively ($p < 0.05$) (Fig. 2, *C* and *D*).

Metformin inhibits T2DM-induced activation of p38 and JNK MAPK but not ERK MAPK

Western blot analyses of pancreatic islets or INS-1 cells were performed using antibodies that react with either the total or phosphorylated of each of the three MAPKs to investigate whether these three MAPKs are activated or inhibited in diabetic pancreas exposure to metformin. The total amount of each MAPK remained constant, p38 and JNK phosphorylation was significantly increased in T2DM group compared with the control group, while metformin reversed the activation of p38 and JNK phosphorylation in diabetic rats in a dose-dependent

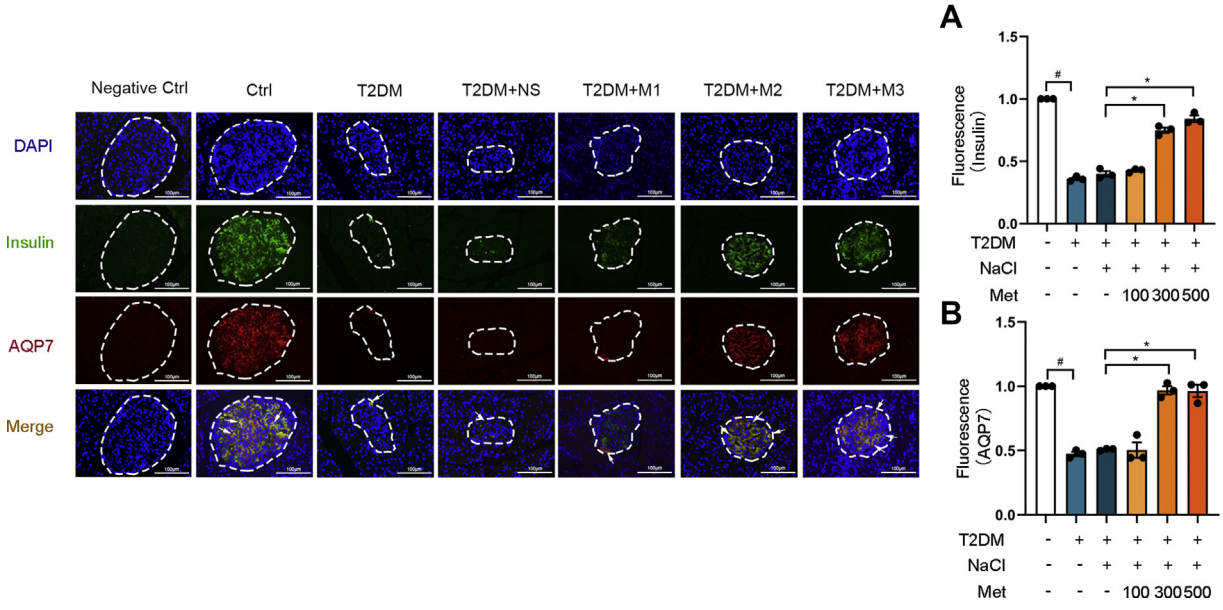

Figure 1. AQP7 expression in pancreatic islets. Double immunofluorescent staining for AQP7 in *red* and insulin (a marker of pancreatic β-cell) in *green* showed AQP7 was colocalized with insulin in *yellow*. *Arrows* show AQP7 detectable in pancreatic β-cell marker. Nuclei are labeled by DAPI in *blue*.*A*, bar graph shows a quantification of insulin fluorescence. *B*, bar graph shows a quantification of AQP7 fluorescence. Control group (Ctrl), untreated diabetic group (T2DM), 0.9% normal saline-treated diabetic group (T2DM+NS), low-dose (100 mg/kg) Met-treated diabetic group (T2DM+M1), middle-dose (300 mg/kg) Met-treated diabetic group (T2DM+M2), high-dose (500 mg/kg) Met-treated diabetic group (T2DM+M3). Results are expressed as Mean ± SEM of three independent experiments. Scale bars = 100 μm, $^{\#}p < 0.05$ *versus* Ctrl group; $^{*}p < 0.05$ *versus* T2DM+NS group.

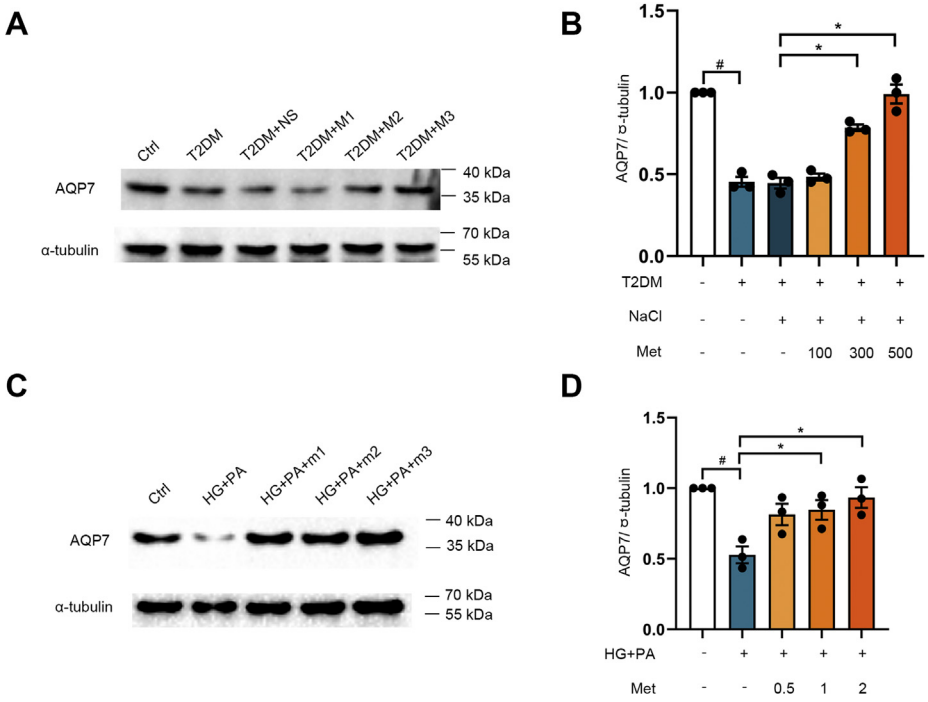

Figure 2. Effect of metformin (Met) on AQP7 protein expression of pancreatic islets or INS-1 cells. *In vivo*, western blot analyses of AQP7 levels in pancreatic islets of the control group (Ctrl), untreated diabetic group (T2DM), 0.9% normal saline-treated diabetic group (T2DM+NS), low-dose (100 mg/kg) Met-treated diabetic group (T2DM+M1); middle-dose (300 mg/kg) Met-treated diabetic group (T2DM+M2), and high-dose (500 mg/kg) Met-treated diabetic group (T2DM+M3). *A*, representative blots for each group are shown; *B*, *bar graph* shows a quantification as AQP7/α-tubulin. Results are expressed as Mean ± SEM of three independent experiments. $^{\#}p < 0.05$ *versus* Ctrl group; $^{*}p < 0.05$ *versus* T2DM+NS group. *In vitro*, western blot analyses of AQP7 levels in INS-1 cells of the control group (Ctrl), 33 mM glucose and 0.25 mM palmitate (HG+PA), 33 mM glucose and 0.25 mM palmitate with 0.5 mM Met group (HG+PA+m1), 1 mM Met group (HG+PA+m2), or 2 mM Met group (HG+PA+m3). *C*, representative blots for each group are shown; *D*, *bar graph* shows a quantification as AQP7/α-tubulin. Results are expressed as Mean ± SEM of three independent experiments. $^{\#}p < 0.05$ *versus* Ctrl group; $^{*}p < 0.05$ *versus* HG+PA group.

manner. However, ERK phosphorylation had no significant changes among different groups ($p < 0.05$) (Fig. 3, *A–F*).

In vitro, after incubation INS-1 cells with 0.25 mM palmitate and 33 mM glucose for 24 h, JNK phosphorylation increased, p38 phosphorylation increased, and ERK MAPK phosphorylation remained unchanged. Furthermore, metformin mostly rescued the activation of JNK and p38 MAPK phosphorylation ($p < 0.05$) (Fig. 4, *A–F*). We also tested the changes in phosphorylated MAPK signaling molecules treated with 0.25 mM palmitate and 33 mM glucose for short time duration (0, 1, 2, 5, 10 and 15 min). The results showed that the phosphorylation levels of JNK and p38 increased after treatment with 33 mM glucose and 0.25 mM palmitate for 1, 2, 5, 10, and 15 min, which were time-dependent. The phosphorylation levels of ERK increased after treatment with 33 mM glucose and 0.25 mM palmitate for 1, 2, and 5 min, but it returned to normal after 10 min (Fig. S2).

Metformin rescues intracellular glycerol content, KCl-stimulated insulin secretion (KSIS), and glucose-stimulated insulin secretion (GSIS) impaired by glucolipotoxicity

Next, we examined the glycerol permeability of each group in INS-1 cells. Glycerol permeability was evaluated by calculating the time course of the intracellular glycerol content change of INS-1 cells subjected to a 50 mM glycerol osmotic shock. As observed, glucolipotoxicity abated glycerol permeability. Under this stress condition, metformin could rescue the inhibitory effect of glucolipotoxicity on glycerol permeability and increase intracellular glycerol content ($p < 0.05$) (Fig. 5*A*).

To determine the effects of glucolipotoxicity on insulin secretion and whether metformin could rescue insulin secretion function in pancreatic β-cells, INS-1 cells were exposed to 0.25 mM palmitate and 33 mM glucose with or without metformin for 24 h. It has shown that KSIS and GSIS were markedly inhibited under the glucolipotoxicity condition. Under the same stress condition, metformin rescued insulin secretion ($p < 0.05$) (Fig. 5*B*).

JNK and p38 MAPKs mediate the expression of AQP7 under glucolipotoxicity condition in INS-1 cells

As shown in Figure 6, SP600125 and SB203580, as inhibitors of JNK and p38, respectively, blocked the decrease of AQP7 protein expression in INS-1 cells after 24 h incubation of 0.25 mM palmitate and 33 mM glucose. Simultaneously, we observed that pharmacological activation of JNK and p38 by anisomycin (a potent agonist of p38 and JNK; 2 μM) also significantly decreased AQP7 protein expression ($p < 0.05$).

Knockdown (KD) or overexpression (OE) of AQP7 alters intracellular glycerol content and insulin secretion in INS-1 cells

To test whether AQP7 was bound to the insulin secretion, we established INS-1 cell lines stably knocking down or

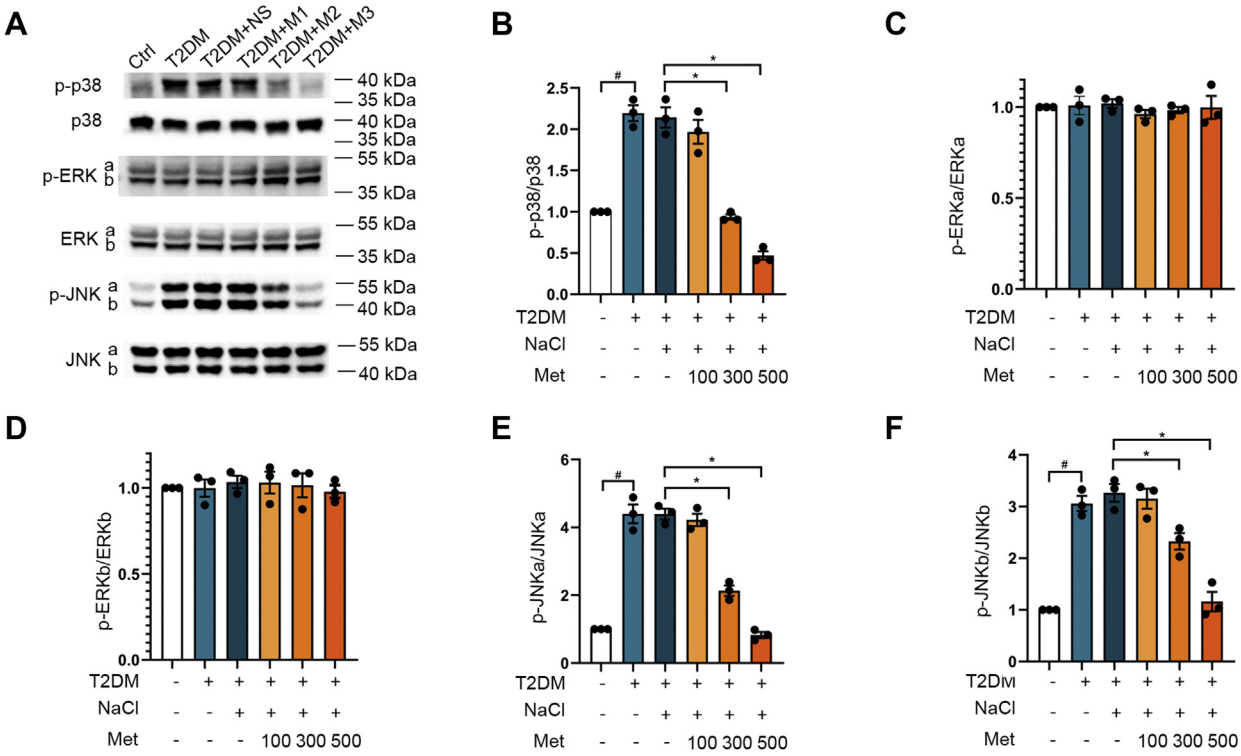

Figure 3. Effects of metformin (Met) on MAPK expression in the pancreatic islets. *A,* the expression of p-p38, p38, p-ERK, ERK, p-JNK, and JNK in the pancreatic islets. *B–F,* the ratio of p-p38/p38, p-ERKa/ERKa, p-ERKb/ERKb, p-JNKa/JNKa and p-JNKb/JNKb in the pancreatic islets, respectively. Control group (Ctrl), untreated diabetic group (T2DM), 0.9% normal saline-treated diabetic group (T2DM+NS), low-dose (100 mg/kg) Met-treated diabetic group (T2DM+M1), middle-dose (300 mg/kg) Met-treated diabetic group (T2DM+M2), high-dose (500 mg/kg) Met-treated diabetic group (T2DM+M3). Results are expressed as Mean ± SEM of three independent experiments. $^{\#}p < 0.05$ *versus* Ctrl group; $^{*}p < 0.05$ *versus* T2DM+NS group.

overexpressing AQP7 by lentiviral infection. The knockdown or overexpression efficiency of AQP7 was substantiated at the protein level using western blot analysis (Fig. 7, *A–D*).

Subsequently, we investigated whether knockdown (KD) or overexpression of AQP7 (OE) could alter glycerol content, insulin secretion in INS-1 cells. The result showed both intracellular glycerol content and insulin secretion were markedly inhibited by AQP7 knockdown (Fig. 7, *E* and *G*). Overexpression of AQP7 could slightly increase the content of intracellular glycerol, but not insulin secretion (Fig. 7, *F* and *H*).

Discussion

In the present study, we demonstrated that a 4-week metformin intervention in T2DM rats ameliorated the metabolic abnormalities induced by hyperglycemia and hyperlipidemia and improved islet cell mass, suggesting that metformin could ameliorate pancreatic islet injury. It was shown that AQP7 expression was decreased, whereas p38 and JNK MAPK were activated in response to hyperglycemia and hyperlipidemia stimuli *in vivo* and *in vitro*. Activation of p38 and JNK MAPK pathway could downregulate AQP7 expression. Furthermore, metformin upregulated AQP7 expression and inhibited p38 and JNK MAPK pathway, implying that metformin might restore AQP7 expression by suppressing specific MAPK pathway so as to provide some protection for rat pancreatic islets. Metformin rescued intracellular glycerol content and insulin secretion impaired by glucolipotoxicity. Overexpression of AQP7 increased glycerol influx into INS-1, and inhibition of AQP7 could reduce glycerol influx into INS-1, thereby decreasing insulin secretion.

Although numerous studies have focused on the roles of metformin in regulating glucose homeostasis and promoting insulin sensitivity, the exact mechanism of metformin on the pancreas remains unclear. Previous studies demonstrated that a decrease in β-cell mass or impaired β-cell function could lead to abnormal plasma insulin levels, thereby promoting glucose intolerance and diabetes (6). The present study showed that metformin alleviated pancreatic islet degeneration and increased β-cell mass in type 2 diabetic rats, suggesting its possible direct protective effect on the pancreas.

Previous experiments using adenovirus-mediated gene transfer of glycerol kinase (Gyk) to insulinoma cell line or isolated rat β-cells showed that proinsulin biosynthesis and insulin secretion stimulated when glycerol is metabolized (5, 16). To date, one of the known mammalian glycerol channels is subcategorized as aquaglyceroporins, which permeate glycerol as well as water, including AQP3, 7, 9, and 10 (17). Among them, AQP7 is a unique aquaglyceroporin in pancreatic islets β-cells (6). Moreover, AQP7 deficiency is associated with a reduction in islet cell number and total β-cell mass (6). Additionally, the human AQP7 gene is in chromosomal region 9p13.3–p21.1 and has been reported being linked

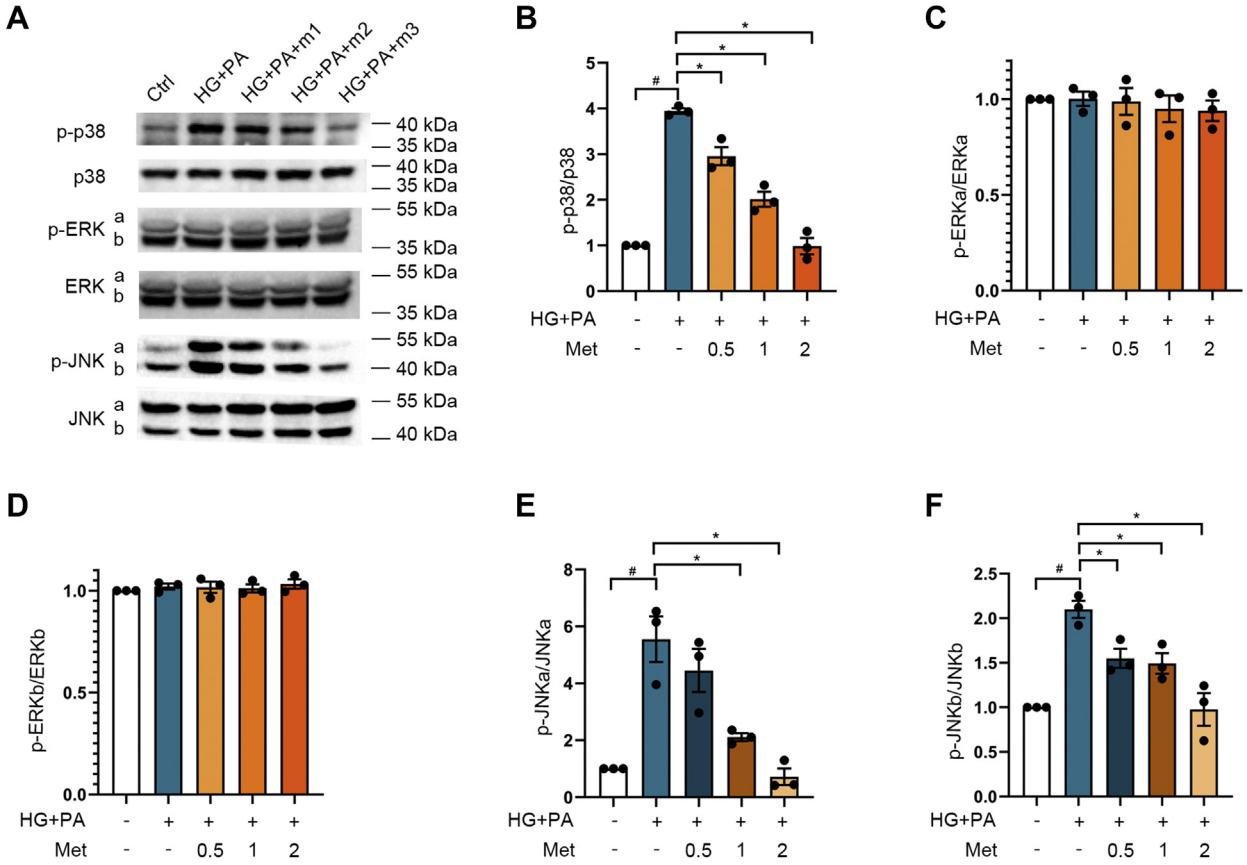

Figure 4. Effects of metformin (Met) on MAPK expression in the INS-1 cells. *A*, the expression of p-p38, p38, p-ERK, ERK, p-JNK, and JNK in the INS-1 cells. *B–F*, the ratio of p-p38/p38, p-ERKa/ERKa, p-ERKb/ERKb, p-JNKa/JNKa and p-JNKb/JNKb in the INS-1 cells, respectively. Results are expressed as Mean ± SEM of three independent experiments. Control group (Ctrl), 33 mM glucose and 0.25 mM palmitate (HG+PA), 33 mM glucose and 0.25 mM palmitate with 0.5 mM Met group (HG+PA+m1), 1 mM Met group (HG+PA+m2), or 2 mM Met group (HG+PA+m3). Results are expressed as Mean ± SEM of three independent experiments. $^{\#}p < 0.05$ *versus* Ctrl group; $^{*}p < 0.05$ *versus* HG+PA group.

to T2DM (18). These studies show that glycerol mediated by AQP7 is involved in glucose metabolism in the pancreas (18). As found in previous studies, AQP7 permeated glycerol influx into β-cell. The present study also demonstrated that shRNA downregulation of AQP7 or hyperglycemia-induced reduction in AQP7 expression could decrease glycerol influx into β-cell,

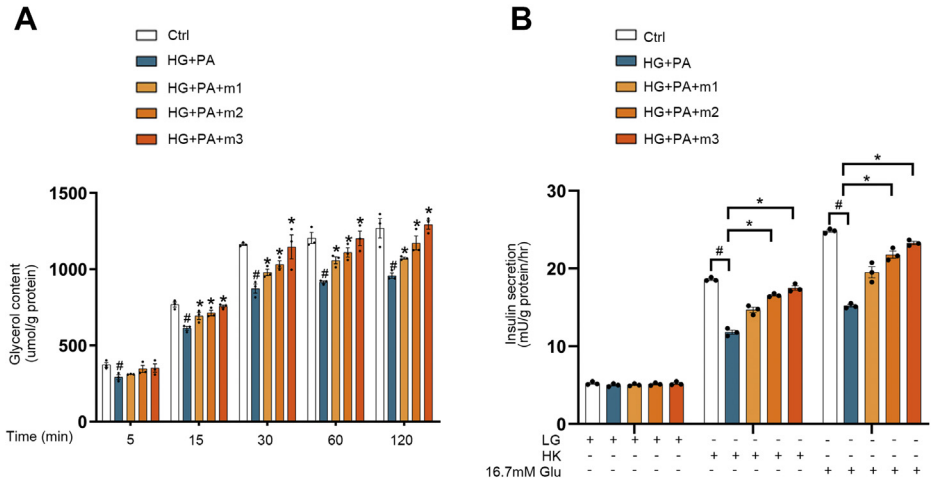

Figure 5. The glycerol content and insulin secretion of INS-1 cells following glucolipotoxicity condition with or without metformin (Met) treatment. *A*, intracellular glycerol levels were measured before and after 5, 15, 30, 60, and 120 min addition of 50 mM glycerol. Control group (Ctrl), 33 mM glucose and 0.25 mM palmitate (HG+PA), 33 mM glucose and 0.25 mM palmitate with 0.5 mM Met group (HG+PA+m1), 1 mM Met group (HG+PA+m2), or 2 mM Met group (HG+PA+m3). Results are expressed as Mean ± SEM of three independent experiments. $^{\#}p < 0.05$ *versus* Ctrl group; $^{*}p < 0.05$ *versus* HG+PA group. *B*, insulin secretion was stimulated by LG, HK or 16.7 mM in INS-1 cells of Ctrl group, HG+PA group, HG+PA+m1 group, HG+PA+m2 group and HG+PA+m3 group. LG: 2.8 mM glucose; HK: 50 mM KCl and 2.8 mM glucose; 16.7 mM Glu: 16.7 mM glucose. Results are expressed as Mean ± SEM of three independent experiments. $^{\#}p < 0.05$ *versus* Ctrl group; $^{*}p < 0.05$ *versus* HG+PA group.

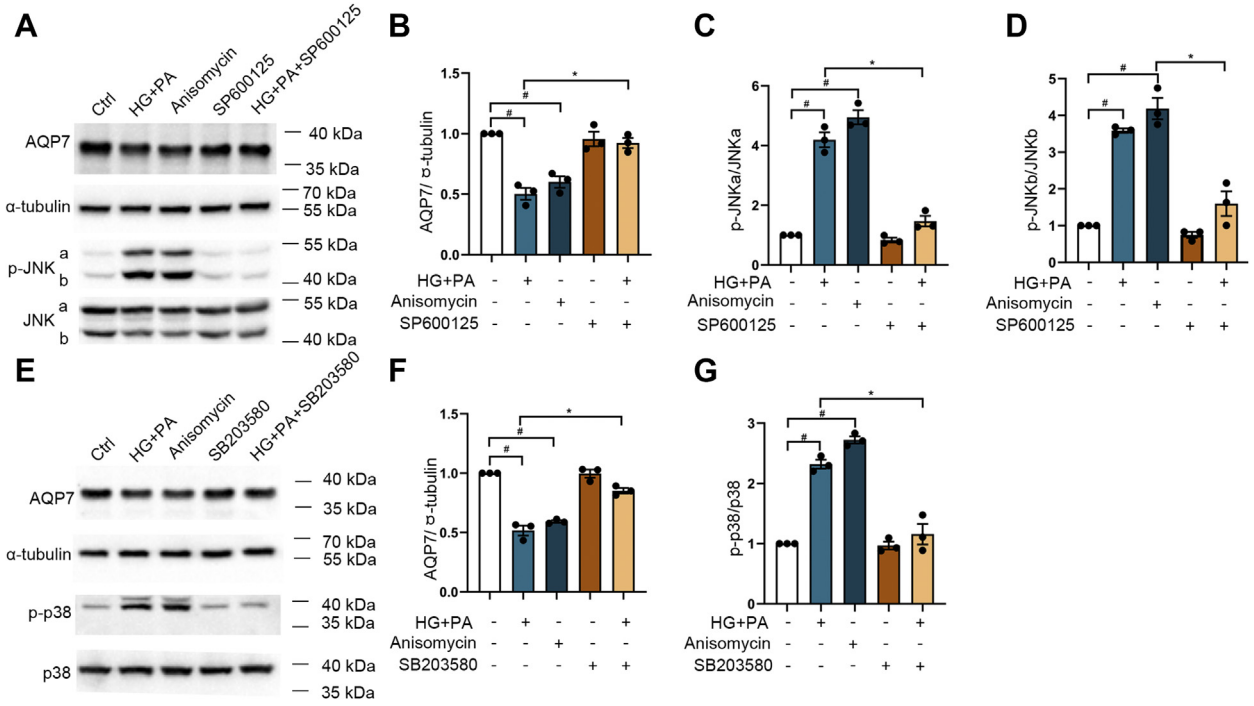

Figure 6. Effects of glucolipotoxicity, Anisomycin, SP600125, SB203580 on the phosphorylation of JNK, p38, and AQP7 in INS-1 cells, detected by western blot. *A*, protein expression of AQP7, phosphorylated JNK (p-JNK) and JNK in INS-1 cells with different treatments (Ctrl, HG+PA, Anisomycin, SP600125 and HG+PA+SP600125). *B*, the proportion of AQP7 in α-tubulin in INS-1 cells. *C*, the ratio of p-pJNKa/JNKa in INS-1 cells. *D*, the ratio of p-pJNKb/JNKb in INS-1 cells. *E*, protein expression of AQP7, p-p38, and p38 in INS-1 cells with different treatments (Ctrl, HG+PA, Anisomycin, SB203580, and HG+PA+SB203580). *F*, the proportion of AQP7 in α-tubulin in INS-1 cells. *G*, the ratio of p-p38/p38 in INS-1 cells. Results are expressed as Mean ± SEM of three independent experiments. Control group (Ctrl), 33 mM glucose and 0.25 mM palmitate (HG+PA), Anisomycin (a potent agonist of p38 and JNK; 2 μM) group (Anisomycin), JNK inhibitor SP600125 (10 μM) group (SP600125), 33 mM glucose +0.25 mM palmitate+10 μM SP600125 group (HG+PA+SP600125), p38 MAPK inhibitor SB203580 (10 μM) group (SB203580), 33 mM glucose +0.25 mM palmitate+10 μM SB203580 group (HG+PA+SB203580). Results are expressed as Mean ± SEM of three independent experiments. $^{\#}p < 0.05$ *versus* Ctrl group; $^{*}p < 0.05$ *versus* HG+PA group.

thereby decreasing insulin secretion. Overexpression of AQP7 induced glycerol influx into β-cell; however, insulin secretion was not increased significantly. The reason for this may be that insulin production is regulated by several pathways except for glycerol. In addition, our data showed that metformin increased intracellular glycerol content, insulin secretion, and upregulated hyperglycemia-induced decrease in AQP7 expression in a dose-dependent manner, indicating that metformin exerts protective effects on the pancreas through modulation of AQP7 expression. Based on the above, our results suggested that upregulation of AQP7 during the metformin treatment of T2DM increased glycerol entering into β-cell, thereby promoting insulin secretion.

The outcome of T2DM therapy largely depends on the complex network of signaling pathways, including activating or inhibiting the specific transcription factors following drug treatment. In present study, we found that metformin inhibits MAPK signaling and rescues pancreatic AQP7 expression to induce insulin secretion in T2DM, suggesting that MAPK may be involved in metformin rescues AQP7 on pancreas. The MAPK family includes a serial cascade that regulates various biological processes in response to a variety of cellular signals, such as insulin signaling (19). The MAPK pathway comprises a core constituted sequentially by JNK (c-Jun N-terminal kinase), ERK1/2 (extracellular signal-regulated kinases 1/2), and p38 (p38 kinase) (19). Some researchers demonstrated that activation of JNK MAPK is relevant for a central signal transduction event promoting peripheral insulin resistance, suppressing insulin production and secretion, and increasing apoptosis of islet cells (20, 21). Other researchers reported that activation of p38 MAPK appears to trigger pancreatic β-cell dysfunction and apoptosis in response to oxidative stress and cytokines *in vitro* (22). Our results were consistent with the reports demonstrating that streptozocin (STZ) combined with high-fat diet activates p38 and JNK MAPK pathway, while ERK MAPK is unaltered (23). However, the changes in ERK MAPK under only hyperglycemia or hyperlipidemia, or hyperglycemia and hyperlipidemia conditions, remain controversial. Previous reports have shown that ERK phosphorylation status remained unchanged under 33 mM glucose stimulus for 48 h in INS-1 cells (8), whereas other studies have shown increased levels of phosphorylation of ERK in cells treated with glucose for short periods of time (16). The present study was consistent with previous studies that ERK was activated in the presence of hyperglycemia and hyperlipidemia during short time stimuli. The inconsistency of ERK changes across studies may be due to different culture conditions or different time duration. The present study also identified that metformin reduced hyperglycemia and hyperlipidemia-induced activation of phosphorylation of p38 and JNK. *In vitro*, it showed similar result that suppressing p38 and JNK MAPK pathway could upregulate AQP7 expression. Furthermore, other researchers and our

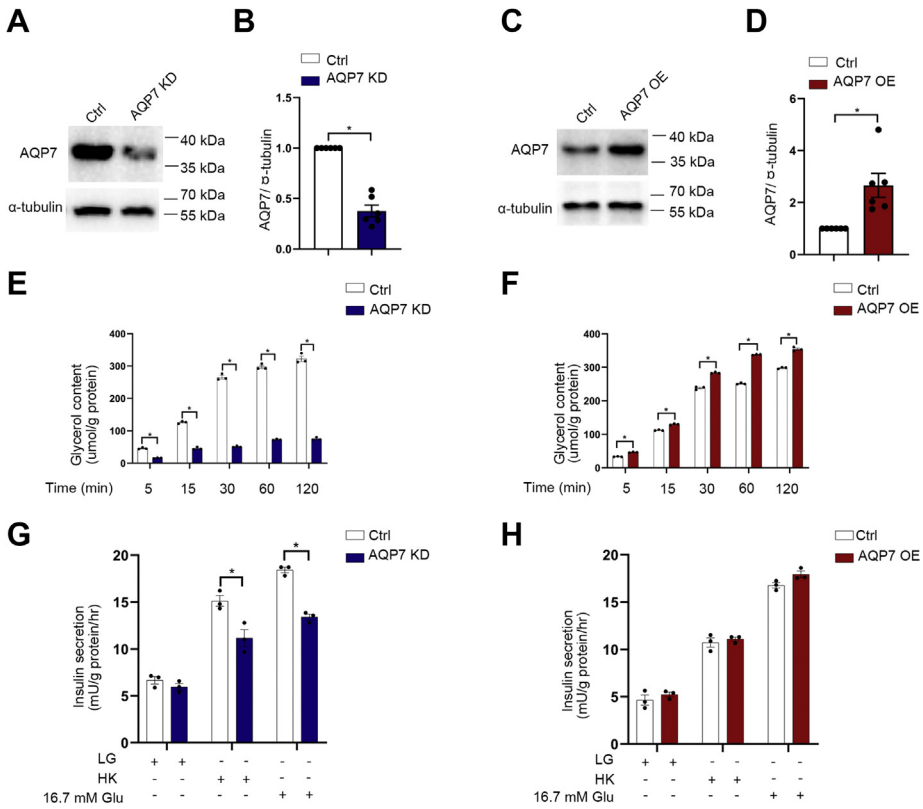

Figure 7. Impact of AQP7 on intracellular glycerol content and insulin secretion in INS-1 cells. AQP7 expression after knockdown (KD) or overexpression (OE) of AQP7 in INS-1 cells (*A* and *C*). *Bar graph* shows a quantification as AQP7/α-tubulin (*B* and *D*). Glycerol content (*E* and *F*) and insulin secretion (*G* and *H*) after knockdown (KD) or overexpression (OE) of AQP7 in INS-1 cells. LG: 2.8 mM glucose; HK: 50 mM KCl and 2.8 mM glucose; 16.7 mM Glu:16.7 mM glucose. Results are expressed as Mean ± SEM of at least three independent experiments. *$p < 0.05$ *versus* Ctrl group.

laboratory demonstrated that MAPK is involved in the regulation of aquaglyceroporin (24–26). Based on the above, we hypothesized that AQP7 is partially mediated *via* MAPKs signal pathway, but does not exclude the existent of other molecules and pathways, *e.g.*, dibutyryl cyclic AMP (27), PKA (28, 29), PKC (30), AMP-activated protein kinase (AMPK) (31), and PI3K/Akt signal transduction pathway in the pancreas (32). Furthermore, other mechanisms might be involved in metformin rescue of pancreatic AQP7. Some studies showed that metformin ameliorates the inhibition of insulin secretion from INS-1 cells under glucotoxic conditions by suppressing the ATP-conducting mitochondrial outer membrane voltage-dependent anion channel-1 (VDAC1) (33) or activating AMPK/sirtuin 1 (SIRT1)/peroxisome proliferator-activated receptor gamma coactivators-1α (PGC-1α) signal pathway (34). Some other studies showed that metformin prevents high-glucose-induced Rac1 [GTP-bound conformation] activation, nuclear translocation, cluster determinant 36 (CD36) expression, and this ultimately prevents high-glucose-induced β-cell dysfunction (35, 36). Whether metformin regulates AQP7 expression through VDAC1, AMPK/SIRT1/PGC-1α, Rac1, CD36, or some other pathway or whether these pathways synergy with the MAPK signal in pancreas, it needs further studies.

In summary, we propose a mechanism by which metformin regulates glucose homeostasis *via* alleviating pancreatic dysfunction in type 2 diabetic rats. This improvement is tightly associated with upregulation of pancreatic AQP7 expression to induce glycerol influx to promote insulin secretion by inhibition of phosphorylation of JNK and p38 MAPK pathway in T2DM (Fig. 8). Our findings indicate that the novel mechanism for metformin treatment of T2DM and the selective modulation of AQP7 function may have important implications for therapeutic strategies of T2DM. Our work should be more informative for studying whether the deficiency of AQP7 could impair the effect of metformin *in vivo*, the effect of metformin on AQPs expression, glycerol flux, and insulin response in other tissues in the future.

Experimental procesures

Ethics statement

This study was explicitly approved by the ethics committees of Chongqing Medical University. All procedures were based on the recommendations of the National Institute of Health (NIH) Guide for the Care and Use of Laboratory Animals (NIH Publications No. 80-23).

Animals

Male Sprague-Dawley rats (200–250 g body weight) were obtained from the Animal Breeding Facility, Chongqing Medical University. Animals were cared for in accordance with the principles of Experimental Animals of Chongqing Medical

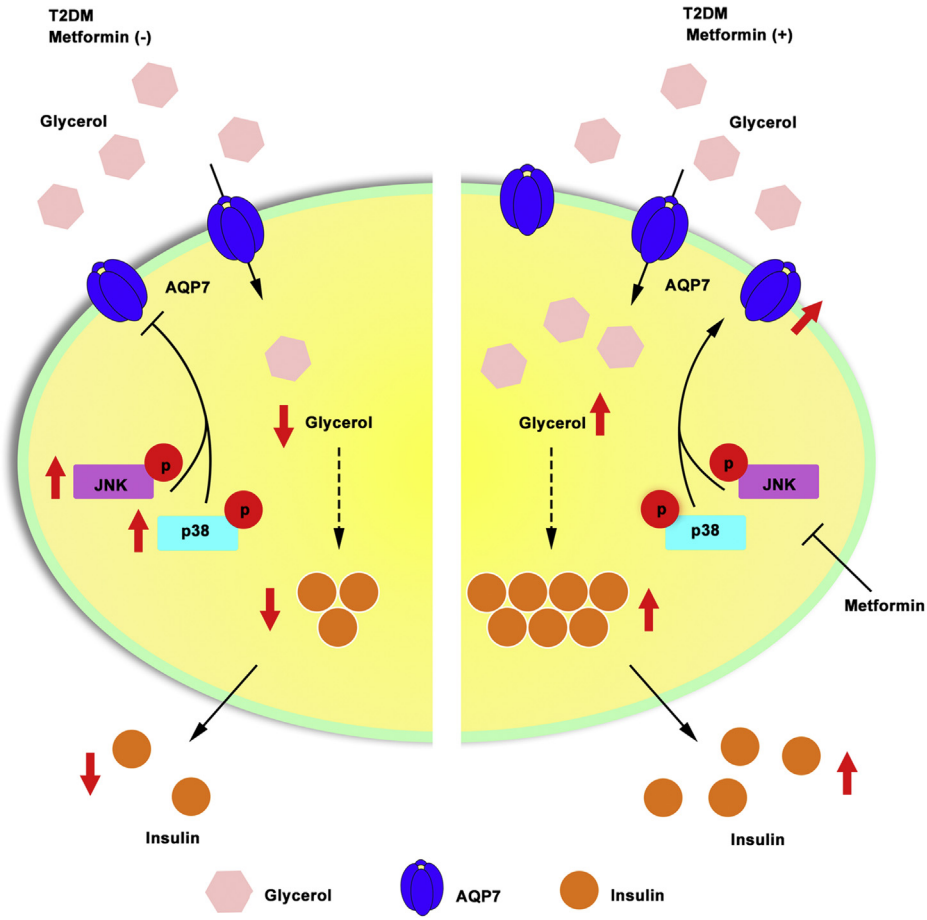

Figure 8. Summary for regulations of metformin on pancreatic β-cells under glucolipotoxicity-challenged. Metformin could suppress p38 and JNK MAPK pathway, thereby upregulate pancreatic AQP7 expression, which facilitates glycerol influx into pancreatic *β*-cell to promote insulin secretion in T2DM.

University. Rats were raised under a 12 h dark–light artificial cycle.

Establishment of type 2 diabetes mellitus

Control Sprague-Dawley rats were fed on a standard chow diet, with an Atwater Fuel Energy of 3.0 kcal/g, comprising 66% calories from carbohydrate, 22% from protein, and 12% from fat. To induce diabetes, Sprague-Dawley rats were fed with the high-fat diet prepared with a total kcal value of 5.3 kcal/g, comprising 60% calories from fat, 35% from protein, and 5% from carbohydrate for 4 weeks (37–39), and then diabetic rats were induced by intraperitoneal injection of 30 mg/kg STZ from Sigma in 0.1 M citrate buffer solution (pH = 4.5). Fasting blood glucose (FBG) levels were measured 72 h after STZ injection by Rightest Glucometer (Bionime Corporation, Taiwan), and diabetic model was considered successfully established in rats with blood glucose levels higher than 16.7 mM. Rats were randomly divided into the normal control group (Ctrl), diabetes mellitus group (T2DM), diabetes mellitus group +0.9% NaCl group (T2DM+NS), and T2DM+Metformin (100, 300, and 500 mg/kg/d) groups. T2DM+Metformin (Met) groups [T2DM+M1 (100 mg/kg/d), T2DM+M2 (300 mg/kg/d), and T2DM+M3 (500 mg/kg/d)] were administered intragastrically with metformin for 4 weeks. T2DM+NS group was treated with an equal volume of 0.9% NaCl.

Pancreatic islet isolation

The pancreatic isolation procedure was carried out under sterile conditions in a biological safety cabinet as before (40, 41). After SD rats were anesthetized with 50 to 75 mg/kg pentobarbital sodium, their abdominal walls were cut open. Ten milliliter Hank's buffered saline solution (HBSS) (Gibco) containing collagenase V (1.0–1.2 mg/ml, Sigma) was injected into the common bile duct of the rat. The pancreas swollen with the digestion solution was quickly excised and immersed into a plastic culture bottle with solution for 13 to 15 min incubation at 37 °C. The digested suspension obtained by shaking the bottle was filtered through 0.5 mm metal mesh and washed with HBSS complement with 2% bovine serum albumin. Islets were obtained from rats by the discontinuous Ficoll density gradient centrifugation.

Cell culture

INS-1 cell line was obtained from the Cell Resource Center, IBMS, CAMS/PUMC. Cells were cultured in Roswell Park Memorial Institute regular RPMI-1640 medium at 11 mM

glucose supplemented with 15% fetal bovine serum (Foundation, Gemini) and 50 μM β-mercaptoethanol at 37 °C in a humidified atmosphere with 5% CO2. For experiments, cells were exposed to for the indicated time. The basal medium glucose concentration was 11 mM glucose when growing INS-1 cells. So the control group cells were cultured in basal medium (absence of palmitate and presence of 11 mM glucose), containing 22 mM mannitol and palmitate solvent. Treatment group cells were incubated in the presence of glucose (33 mM) and palmitate (0.25 mM) with or without metformin. For signal pathway study, cells were pretreated with the JNK inhibitor SP600125 (10 μM) or the p38 MAPK inhibitor SB203580 (10 μM) for 1 h or pretreated with anisomycin (a potent agonist of p38 and JNK; 2 μM) (23, 42) for 2 h before 0.25 mM palmitate and 33 mM glucose treatment.

Western blot analysis

Pancreatic tissues and INS-1 cells were homogenized in RIPA lysis buffer (Beyotime Institute of Biotechnology) containing protease and phosphatase inhibitor cocktails in the lysis buffer. Protein concentrations of the homogenates were measured by a BCA protein assay kit (Beyotime Institute of Biotechnology). The extracted proteins (50 μg) were separated by 10% SDS–PAGE gels and then transferred onto membranes. Blotted membranes of phosphorylated proteins were blocked with 5% bovine serum albumin (5% BSA) and blotted membranes of nonphosphorylated proteins were blocked with 5% skimmed milk. After blocking, the membranes were then incubated with primary antibody against AQP7 (SC376407, 1:200, mouse anti-AQP7; Santa Cruz), or p38 (66234-1-lg, 1:1000, mouse anti-p38; Proteintech), or phosphorylated p38 (#4511, 1:1000, rabbit anti-p-p38; Cell Signaling Technology), or ERK1/2 (67170-1-Ig, 1:1000, mouse anti-ERK; Proteintech), or phosphorylated ERK1/2 (#4370, 1:1000, rabbit anti-p-ERK1/2; Cell Signaling Technology), or JNK (66210-1-lg, 1:1000, mouse anti-JNK; Proteintech), or phosphorylated JNK (#4668, 1:1000, rabbit anti-p- JNK; Cell Signaling Technology), or α-tubulin (66031-1-lg, 1:5000, mouse anti-α-tubulin; Proteintech). After that, the membranes were incubated with horseradish-peroxidase-conjugated secondary antibody (goat anti-rabbit HRP or goat anti-mouse HRP, ZSGB-Bio). The specific reaction was visualized by a chemiluminescent substrate (ECL). The bands were quantified by densitometry using gel densitometry (quantity one) software. Results were expressed as AQP7/α-tubulin, p-MAPK/MAPK. Each point was repeated in triplicate.

Immunofluorescence staining

Rats were deeply anesthetized and then perfused transcardially using 4 °C normal saline, followed by fixation with 4% paraformaldehyde in 0.1 M PBS. Pancreatic tissues were removed and placed in 30% sucrose-PBS overnight. Tissues were then sliced (10 μm thickness). Sections were washed with 0.01 M PBS, incubated with 0.2% Triton X-100 and 4% horse serum (HS), and blocked with 4% HS for 60 min. Sections were then incubated overnight at 4 °C with primary antibodies specific for AQP7 (SC376407, 1:50, mouse anti-AQP7; Santa Cruz) mixed with insulin (H-86) (AF5109, 1:100, rabbit anti-insulin; Affinity Biosciences). Afterward, sections were incubated for 1 h at room temperature with fluorescein Alex488-labeled anti-rabbit IgG mixed with Cy3-labeled anti-mouse IgG (Beyotime Institute of Biotechnology). Nuclei were labeled with 4′, 6-diamidino-2-phenylindole (1 mg/ml) for 5 min at room temperature. Sections were mounted in glycerol and visualized by a fluorescence microscope (Leica).

KSIS assay and GSIS assay

INS-1 cells were cultured in 6-well plates with the corresponding treatments KSIS and GSIS assays. INS-1 cells were preincubated for 1 h in Kreb's ringer bicarbonate (KRB) buffer (137 mM NaCl, 4.7 mM KCl, 2.5 mM CaCl2, 1.2 mM MgSO4, 1.2 mM KH2PO4, 25 mM NaHCO3, and 1% BSA) (pH 7.4) containing 2.8 mM glucose. Then, INS-1 cells were incubated for 1 h in KRB buffer containing basal glucose (LG: 2.8 mM) or in KRB buffer containing stimulatory condition 50 mM KCl and 2.8 mM glucose (HK) or 16.7 mM glucose (16.7 mM Glu). The supernatants were obtained, after the static incubation period. After treatment, cell supernatants were collected and secreted insulin was measured by using the Rat Insulin Enzyme-linked immunosorbent assay (ELISA) Kit (JM-01993R1, Jiangsu Jingmei Biotechnology Co, Ltd) according to the instructions.

Measurement of glycerol content

INS-1 cells cultured in 6-well plates were exposed to glucose (33 mM) and palmitate (0.25 mM) with or without metformin, and then the medium was aspirated and replaced with 50 mM glycerol for exactly 0, 5, 15, 30, 60, and 120 min. The reactions were terminated and the excess glycerol was removed with three washes of ice-cold PBS. Intracellular glycerol levels were measured by a quantitative enzymatic determination glycerol assay kit (Applygen Technologies Inc).

Lentivirus infection

Lentivirus infection for the INS-1 cells was conducted as described previously (43). Briefly, to establish INS-1 cells with stable AQP7 overexpression, the Ubi-AQP7-MCS-3FLAG-SV40-EGFP-IRES-puromycin lentivirus, which encodes a full-length rat AQP7 gene, and the Ubi-MCS-3FLAG-SV40-EGFP-IRES-puromycin as empty vector control were transfected into INS-1 cells, and stable clones with AQP7 overexpression were selected after 2 weeks with 0.5 to 2 μg/ml puromycin. The hU6-AQP7-MCS-CBh-gcGFP-IRES-puromycin lentivirus containing the target sequences (5′-CTGCAGCTACCACCTACTTAA -3′) was used for AQP7 knockdown and the negative control was the hU6-MCS-CBh-gcGFP-IERS-puromycin with its sequences as follows: 5′-TTCTCCGAACGTGTCACGT -3′. After transfection, cells were harvested and the knockdown or overexpression efficiency was determined using western blot. The vector constructions (verification by Sanger sequencing), virus packaging,

and collection of the corresponding viral supernatants were performed by GeneChem Co, Ltd.

Statistical analysis

All data were presented as Mean ± SEM, and p value was analyzed by Student's t test or ANOVA. Values of $p < 0.05$ were considered statistically significant.

Data availability

All data are indicated in the manuscript.

Supporting information—This article contains supporting information.

Author contributions—X. H., T. L., J. T., X. L., and M. W. data curation; X. H., J. H., and X. L. formal analysis; M. Y. funding acquisition; F. G. and M. Y. investigation; X. H. and M. W. methodology; F. G. and M. Y. project administration; X. H., J. H., C. W., X. L., H. L., and Y. C. resources; X. H., F. G., T. L., and H. L. software; Y. C. supervision; J. H. validation; T. L. visualization; F. G. and J. H. writing—original draft; Z. Y. and M. Y. writing—review and editing.

Funding and additional information—Funding from the National Natural Science Foundation of China (81971230 and 81671312), Science and technology research project of Chongqing Education Commission (KJQN201800428) to M. Y.; National Natural Science Foundation of China (81672893), Senior Young-middle-aged Medical Talents Program of Chongqing Health Committee (No.204216qn), Chongqing Science and Health Joint Project (2020GDRC007) and Reserve Talents Program for academic Leaders of the First Affiliated Hospital of Chongqing Medical University (No.XKTS070) to F. G.

Conflict of interest—The authors declare that they have no conflict of interest associated with this study.

Abbreviations—The abbreviations used are: AMPK, AMP-activated protein kinase; AQP7, aquaporin 7; CD36, cluster determinant 36; ERK1/2, extracellular signal-regulated kinases 1/2; FBG, fasting blood glucose; Glu, glucose; GSIS, glucose-stimulated insulin secretion; HE, hematoxylin and eosin; JNK, c-Jun N-terminal kinase; KD, knockdown; KSIS, KCl-stimulated insulin secretion; MAPK, mitogen-activated protein kinase; OE, overexpression; PGC-1α, peroxisome proliferator-activated receptor gamma coactivators-1α; T2DM, type 2 diabetes mellitus; TC, total cholesterol; TG, triglyceride; VDAC1, voltage-dependent anion channel-1.

References

1. Bailey, C. J., and Turner, R. C. (1996) Metformin. *N. Engl. J. Med.* **334**, 574–579
2. Kirpichnikov, D., McFarlane, S. I., and Sowers, J. R. (2002) Metformin: An update. *Ann. Intern. Med.* **137**, 25–33
3. Matthaei, S., Stumvoll, M., Kellerer, M., and Haring, H. U. (2000) Pathophysiology and pharmacological treatment of insulin resistance. *Endocr. Rev.* **21**, 585–618
4. Yang, X., Xu, Z., Zhang, C., Cai, Z., and Zhang, J. (2016) Metformin, beyond an insulin sensitizer, targeting heart and pancreatic beta cells. *Biochim. Biophys. Acta Mol. Basis Dis.* **1863**, 1984–1990
5. Skelly, R. H., Wicksteed, B., Antinozzi, P. A., and Rhodes, C. J. (2001) Glycerol-stimulated proinsulin biosynthesis in isolated pancreatic rat islets via adenoviral-induced expression of glycerol kinase is mediated via mitochondrial metabolism. *Diabetes* **50**, 1791–1798
6. Matsumura, K., Chang, B. H., Fujimiya, M., Chen, W., Kulkarni, R. N., Eguchi, Y., Kimura, H., Kojima, H., and Chan, L. (2007) Aquaporin 7 is a beta-cell protein and regulator of intraislet glycerol content and glycerol kinase activity, beta-cell mass, and insulin production and secretion. *Mol. Cell. Biol.* **27**, 6026–6037
7. Galant, D., Gaborit, B., Desgrouas, C., Abdesselam, I., Bernard, M., Levy, N., Merono, F., Coirault, C., Roll, P., Lagarde, A., Bonello-Palot, N., Bourgeois, P., Dutour, A., and Badens, C. (2016) A heterozygous ZMPSTE24 mutation associated with severe metabolic syndrome, ectopic fat accumulation, and dilated cardiomyopathy. *Cells* **5**, 21
8. de Gonzalo-Calvo, D., Kenneweg, F., Bang, C., Toro, R., van der Meer, R. W., Rijzewijk, L. J., Smit, J. W., Lamb, H. J., Llorente-Cortes, V., and Thum, T. (2016) Circulating long-non coding RNAs as biomarkers of left ventricular diastolic function and remodelling in patients with well-controlled type 2 diabetes. *Sci. Rep.* **6**, 37354
9. Cristobal, I., Madoz-Gurpide, J., Rojo, F., and Garcia-Foncillas, J. (2016) Comment on Goldsworthy et al. Haploinsufficiency of the insulin receptor in the presence of a splice-site mutation in Ppp2r2a results in a novel digenic mouse model of type 2 diabetes. Diabetes 2016;65:1434-1446. *Diabetes* **65**, e22–e23
10. Lawrence, M. C., Borenstein-Auerbach, N., McGlynn, K., Kunnathodi, F., Shahbazov, R., Syed, I., Kanak, M., Takita, M., Levy, M. F., and Nazir-uddin, B. (2015) NFAT targets signaling molecules to gene promoters in pancreatic beta-cells. *Mol. Endocrinol.* **29**, 274–288
11. Sidarala, V., and Kowluru, A. (2017) The regulatory roles of mitogen-activated protein kinase (MAPK) pathways in health and diabetes: Lessons learned from the pancreatic beta-cell. *Recent Pat. Endocr. Metab. Immune Drug Discov.* **10**, 76–84
12. Yang, G., Yang, W., Wu, L., and Wang, R. (2007) H2S, endoplasmic reticulum stress, and apoptosis of insulin-secreting beta cells. *J. Biol. Chem.* **282**, 16567–16576
13. Li, Z., Liu, H., Niu, Z., Zhong, W., Xue, M., Wang, J., Yang, F., Zhou, Y., Zhou, Y., Xu, T., and Hou, J. (2018) Temporal proteomic analysis of pancreatic β-cells in response to lipotoxicity and glucolipotoxicity. *Mol. Cell. Proteomics* **17**, 2119–2131
14. Guo, L., Liu, J., Zheng, X., Yin, Z., Kosaraju, J., and Tam, K. (2017) Geniposide improves insulin production and reduces apoptosis in high glucose-induced glucotoxic insulinoma cells. *Eur. J. Pharm. Sci.* **110**, 70–76
15. Dai, Y., Huang, S., and Leng, Y. (2015) AICAR and metformin exert AMPK-dependent effects on INS-1E pancreatic β-cell apoptosis via differential downstream mechanisms. *Int. J. Biol. Sci.* **11**, 1272–1280
16. Noel, R. J., Antinozzi, P. A., McGarry, J. D., and Newgard, C. B. (1997) Engineering of glycerol-stimulated insulin secretion in islet beta cells. Differential metabolic fates of glucose and glycerol provide insight into mechanisms of stimulus-secretion coupling. *J. Biol. Chem.* **272**, 18621–18627
17. Rodriguez, A., Catalan, V., Gomez-Ambrosi, J., and Fruhbeck, G. (2011) Aquaglyceroporins serve as metabolic gateways in adiposity and insulin resistance control. *Cell Cycle* **10**, 1548–1556
18. Prudente, S., Flex, E., Morini, E., Turchi, F., Capponi, D., De Cosmo, S., Tassi, V., Guida, V., Avogaro, A., Folli, F., Maiani, F., Frittitta, L., Dallapiccola, B., and Trischitta, V. (2007) A functional variant of the adipocyte glycerol channel aquaporin 7 gene is associated with obesity and related metabolic abnormalities. *Diabetes* **56**, 1468–1474
19. Tang, X., Deng, L., Xiong, H., Li, G., Lin, J., Liu, S., Xie, J., Liu, J., Kong, F., Tu, G., Peng, H., and Liang, S. (2014) Expression profile of mitrogen-activated protein kinase (MAPK) signaling genes in the skeletal muscle & liver of rat with type 2 diabetes: Role in disease pathology. *Indian J. Med. Res.* **140**, 744–755
20. Hirosumi, J., Tuncman, G., Chang, L., Gorgun, C. Z., Uysal, K. T., Maeda, K., Karin, M., and Hotamisligil, G. S. (2002) A central role for JNK in obesity and insulin resistance. *Nature* **420**, 333–336
21. Kaneto, H., Nakatani, Y., Miyatsuka, T., Kawamori, D., Matsuoka, T. A., Matsuhisa, M., Kajimoto, Y., Ichijo, H., Yamasaki, Y., and Hori, M. (2004)

Possible novel therapy for diabetes with cell-permeable JNK-inhibitory peptide. *Nat. Med.* **10**, 1128–1132
22. Makeeva, N., Myers, J. W., and Welsh, N. (2006) Role of MKK3 and p38 MAPK in cytokine-induced death of insulin-producing cells. *Biochem. J.* **393**, 129–139
23. Wang, C., Zou, S., Cui, Z., Guo, P., Meng, Q., Shi, X., Gao, Y., Yang, G., and Han, Z. (2015) Zerumbone protects INS-1 rat pancreatic beta cells from high glucose-induced apoptosis through generation of reactive oxygen species. *Biochem. Biophys. Res. Commun.* **460**, 205–209
24. Wei, X., Ren, X., Jiang, R., Li, H., Gao, F., Chen, Y., Hou, J., Liu, X., Sun, S., and Yang, M. (2015) Phosphorylation of p38 MAPK mediates aquaporin 9 expression in rat brains during permanent focal cerebral ischaemia. *J. Mol. Histol.* **46**, 273–281
25. Arima, H., Yamamoto, N., Sobue, K., Umenishi, F., Tada, T., Katsuya, H., and Asai, K. (2003) Hyperosmolar mannitol simulates expression of aquaporins 4 and 9 through a p38 mitogen-activated protein kinase-dependent pathway in rat astrocytes. *J. Biol. Chem.* **278**, 44525–44534
26. Li, F. X., Huang, L. Z., Dong, C., Wang, J. P., Wu, H. J., and Shuang, S. M. (2015) Down-regulation of aquaporin3 expression by lipopolysaccharide via p38/c-Jun N-terminal kinase signalling pathway in HT-29 human colon epithelial cells. *World J. Gastroenterol.* **21**, 4547–4554
27. Grether-Beck, S., Felsner, I., Brenden, H., Kohne, Z., Majora, M., Marini, A., Jaenicke, T., Rodriguez-Martin, M., Trullas, C., Hupe, M., Elias, P. M., and Krutmann, J. (2012) Urea uptake enhances barrier function and antimicrobial defense in humans by regulating epidermal gene expression. *J. Invest. Dermatol.* **132**, 1561–1572
28. Miyauchi, T., Yamamoto, H., Abe, Y., Yoshida, G. J., Rojek, A., Sohara, E., Uchida, S., Nielsen, S., and Yasui, M. (2015) Dynamic subcellular localization of aquaporin-7 in white adipocytes. *FEBS Lett.* **589**, 608–614
29. Hansen, J. S., Krintel, C., Hernebring, M., Haataja, T. J., de Mare, S., Wasserstrom, S., Kosinska-Eriksson, U., Palmgren, M., Holm, C., Stenkula, K. G., Jones, H. A., and Lindkvist-Petersson, K. (2016) Perilipin 1 binds to aquaporin 7 in human adipocytes and controls its mobility via protein kinase A mediated phosphorylation. *Metab. Clin. Exp.* **65**, 1731–1742
30. Tan, Y. J., Zhang, X. Y., Ding, G. L., Li, R., Wang, L., Jin, L., Lin, X. H., Gao, L., Sheng, J. Z., and Huang, H. F. (2015) Aquaporin7 plays a crucial role in tolerance to hyperosmotic stress and in the survival of oocytes during cryopreservation. *Sci. Rep.* **5**, 17741
31. Kong, C. S., Kim, J. A., Bak, S. S., Byun, H. G., and Kim, S. K. (2011) Anti-obesity effect of carboxymethyl chitin by AMPK and aquaporin-7 pathways in 3T3-L1 adipocytes. *J. Nutr. Biochem.* **22**, 276–281
32. Rodriguez, A., Catalan, V., Gomez-Ambrosi, J., Garcia-Navarro, S., Rotellar, F., Valenti, V., Silva, C., Gil, M. J., Salvador, J., Burrell, M. A., Calamita, G., Malagon, M. M., and Fruhbeck, G. (2011) Insulin- and leptin-mediated control of aquaglyceroporins in human adipocytes and hepatocytes is mediated via the PI3K/Akt/mTOR signaling cascade. *J. Clin. Endocrinol. Metab.* **96**, E586–E597
33. Zhang, E., Mohammed Al-Amily, I., Mohammed, S., Luan, C., Asplund, O., Ahmed, M., Ye, Y., Ben-Hail, D., Soni, A., Vishnu, N., Bompada, P., De Marinis, Y., Groop, L., Shoshan-Barmatz, V., Renström, E., *et al.* (2019) Preserving insulin secretion in diabetes by inhibiting VDAC1 overexpression and surface translocation in β cells. *Cell Metab.* **29**, 64–77.e66
34. Li, Q., Jia, S., Xu, L., Li, B., and Chen, N. (2019) Metformin-induced autophagy and irisin improves INS-1 cell function and survival in high-glucose environment via AMPK/SIRT1/PGC-1α signal pathway. *Food Sci. Nutr.* **7**, 1695–1703
35. Baidwan, S., Chekuri, A., Hynds, D., and Kowluru, A. (2017) Glucotoxicity promotes aberrant activation and mislocalization of Ras-related C3 botulinum toxin substrate 1 [Rac1] and metabolic dysfunction in pancreatic islet β-cells: Reversal of such metabolic defects by metformin. *Apoptosis* **22**, 1380–1393
36. Moon, J., Karunakaran, U., Elumalai, S., Lee, I., Lee, H., Kim, Y., and Won, K. (2017) Metformin prevents glucotoxicity by alleviating oxidative and ER stress-induced CD36 expression in pancreatic beta cells. *J. Diabetes Complications* **31**, 21–30
37. Mansor, L. S., Gonzalez, E. R., Cole, M. A., Tyler, D. J., and Heather, L. C. (2013) Cardiac metabolism in a new rat model of type 2 diabetes using high-fat diet with low dose streptozotocin. *Cardiovasc. Diabetol.* **12**, 136
38. Srinivasan, K., Viswanad, B., Asrat, L., Kaul, C. L., and Ramarao, P. (2005) Combination of high-fat diet-fed and low-dose streptozotocin-treated rat: A model for type 2 diabetes and pharmacological screening. *Pharmacol. Res.* **52**, 313–320
39. Reed, M. J., Meszaros, K., Entes, L. J., Claypool, M. D., Pinkett, J. G., Gadbois, T. M., and Reaven, G. M. (2000) A new rat model of type 2 diabetes: The fat-fed, streptozotocin-treated rat. *Metab. Clin. Exp.* **49**, 1390–1394
40. Veroux, M., Bottino, R., Santini, R., Bertera, S., and Vanella, L. (2019) Mesenteric lymph nodes as alternative site for pancreatic islet transplantation in a diabetic rat model. *BMC Surg.* **18**, 126
41. Tian, J. Y., Guo, L. I., Yan-Yun, G. U., Zhang, H. L., Zhou, W. Z., Wang, X., Zhu, H. D., Luo, T. H., and Luo, M. (2006) Role and mechanism of rosiglitazone on the impairment of insulin secretion induced by free fatty acids on isolated rat islets. *Chin. Med. J.* **119**, 574–580
42. Zhang, X., He, C., Tian, K., Li, P., Su, H., and Wan, J. (2015) Ginsenoside Rb1 attenuates angiotensin II-induced abdominal aortic aneurysm through inactivation of the JNK and p38 signaling pathways. *Vasc. Pharmacol.* **73**, 86–95
43. Li, W., Yan, Y., Zheng, Z., Zhu, Q., Long, Q., Sui, S., Luo, M., Chen, M., Li, Y., Hua, Y., Deng, W., Lai, R., and Li, L. (2020) Targeting the NCOA3-SP1-TERT axis for tumor growth in hepatocellular carcinoma. *Cell Death Dis.* **11**, 1011